Title

Synthesis, Detection, and Metabolism of Pyridone Ribosides, Products of NAD Overoxidation.

Journal

Chemical Research in Toxicology, 37(2)

Authors

Hayat, Faisal

Deason, J

Bryan, Ru

et al.

Publication Date

2024-02-19

DOI

10.1021/acs.chemrestox.3c00264

Peer reviewed

Chemical Research in Toxicology

pubs.acs.org/crt

Article

Synthesis, Detection, and Metabolism of Pyridone Ribosides, Products of NAD Overoxidation

Faisal Hayat, J. Trey Deason, Ru Liu Bryan, Robert Terkeltaub, Weidan Song, W. Lee Kraus, Janice Pluth, Natalie R. Gassman, and Marie E. Migaud*

Cite This: *Chem. Res. Toxicol.* 2024, 37, 248−258

Read Online

ACCESS | Metrics & More | Article Recommendations | Supporting Information

ABSTRACT: Pyridone-containing adenine dinucleotides, ox-NAD, are formed by overoxidation of nicotinamide adenine dinucleotide (NAD^+) and exist in three distinct isomeric forms. Like the canonical nucleosides, the corresponding pyridone-containing nucleosides (PYR) are chemically stable, biochemically versatile, and easily converted to nucleotides, di- and triphosphates, and dinucleotides. The 4-PYR isomer is often reported with its abundance increasing with the progression of metabolic diseases, age, cancer, and oxidative stress. Yet, the pyridone-derived nucleotides are largely under-represented in the literature. Here, we report the efficient synthesis of the series of ox-NAD and pyridone nucleotides and measure the abundance of ox-NAD in biological specimens using liquid chromatography coupled with mass spectrometry (LC-MS). Overall, we demonstrate that all three forms of PYR and ox-NAD are found in biospecimens at concentrations ranging from nanomolar to midmicromolar and that their presence affects the measurements of NAD(H) concentrations when standard biochemical redox-based assays are applied. Furthermore, we used liver extracts and ^{1}H NMR spectrometry to demonstrate that each ox-NAD isomer can be metabolized to its respective PYR isomer. Together, these results suggest a need for a better understanding of ox-NAD in the context of human physiology since these species are endogenous mimics of NAD^+, the key redox cofactor in metabolism and bioenergetics maintenance.

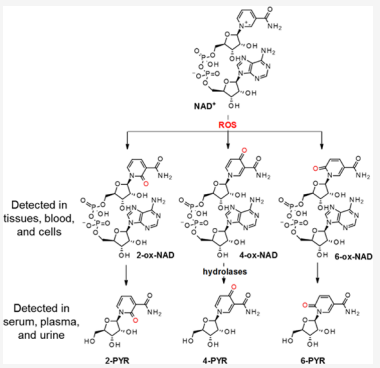

INTRODUCTION

Nicotinamide adenine dinucleotide (NAD^+) and its phosphorylated form ($NADP^+$) play a fundamental role in all forms of life, carrying reducing equivalents (H^-) for anabolic and catabolic processes via interconversion with their respective reduced forms, NADH and NADPH, referred to as NAD(H) and NADP(H), respectively.[1] These redox pairs are essential for many biochemical reactions, generating cellular energy through adenosine triphosphate (ATP). In addition to reversible redox chemistry on the pyridinium ring, NAD(P) is involved in nonreversible processes that release nicotinamide.[2] Nicotinamide can be recycled to NAD^+ or methylated. *N*-methyl-nicotinamide (*N*-Me-Nam) is then oxidized to *N*-methylated pyridones. These *N*-methylated pyridones are the *N*-methyl-2-pyridone-3-carboxamide (Figure 1, *N*-Me-2-PY), *N*-methyl-4-pyridone-3-carboxamide (*N*-Me-4-PY, also named 1-methyl-4-oxopyridine-3-carboxamide, Figure 1), and *N*-methyl-3-carboxamide-6-pyridone (*N*-Me-6-PY, also named 1-methyl-6-oxopyridine-3-carboxamide, but more widely known as *N*-methyl-2-pyridone-5-carboxamide, Figure 1).[3] The latter, along with methyl-*N*-nicotinamide and nicotinuric acid, is the most predominantly reported end product of NAD^+ catabolism found in human biospecimens.[4]

To avoid nomenclature confusion, the numbering of the carboxamide position on the pyridinyl ring remains constant in all forward abbreviations. Other catabolites of nicotinamide include nicotinamide *N*-oxide and 6-hydroxynicotinamide, also known as 6-oxopyridine-3-carboxamide (6-PY, Figure 1), the nonmethylated form of *N*-Me-6-PY. Additional NAD^+ urinary metabolites include the ribosylated forms of these PY nucleobases, the pyridone ribosides (Figure 1, PYRs).[5−8] While less abundant than *N*-Me-PYs, carboxamide pyridone ribosides (PYRs) have been detected numerous times in mammalian urine since the 1970s.[9] Yet, the metabolomics literature often only reports on the 1-ribosylpyridin-4-one-3-carboxamide (4-PYR; Figure 1) species (e.g., ref 10). The triphosphate form of 4-PYR has been formally characterized from blood specimens, and its abundance correlates with chronic kidney disease and kidney failure.[11−14]

A biochemical relationship between the *N*-methylated (*N*-Me-PYs) and *N*-ribosylated (PYRs) has been proposed but not substantiated.[11,14] We posit that such a relationship does not exist, but instead that ribosylated pyridone species are generated by oxidation of the ribosylated forms of nicotinamide by reactive oxygen species, including that of

Received: August 30, 2023
Revised: December 23, 2023
Accepted: December 27, 2023
Published: January 10, 2024

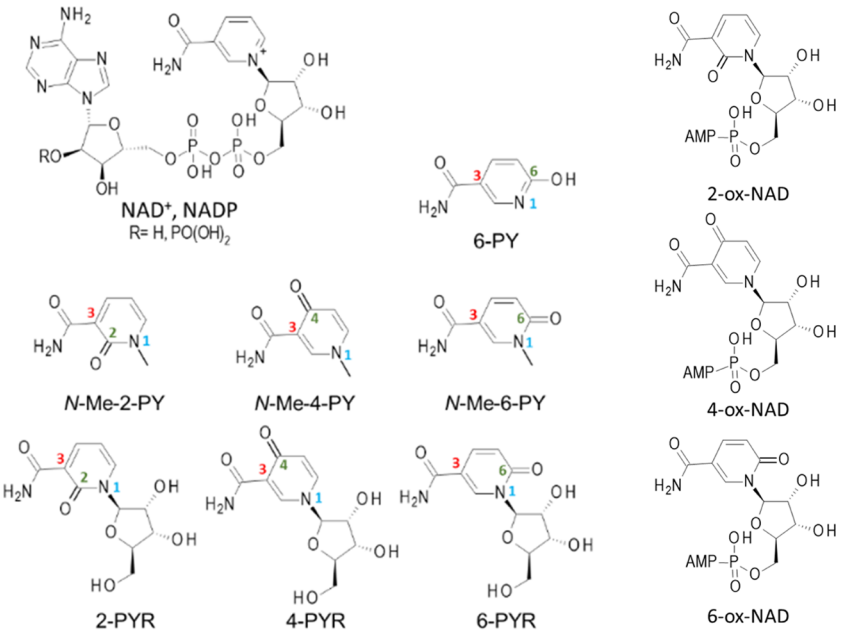

Figure 1. Chemical structures of NAD^+, NADP, pyridones (PYs), methylated pyridones (*N*-Me-PYs), ribosylated pyridones (PYRs), and overoxidized NAD (ox-NAD).

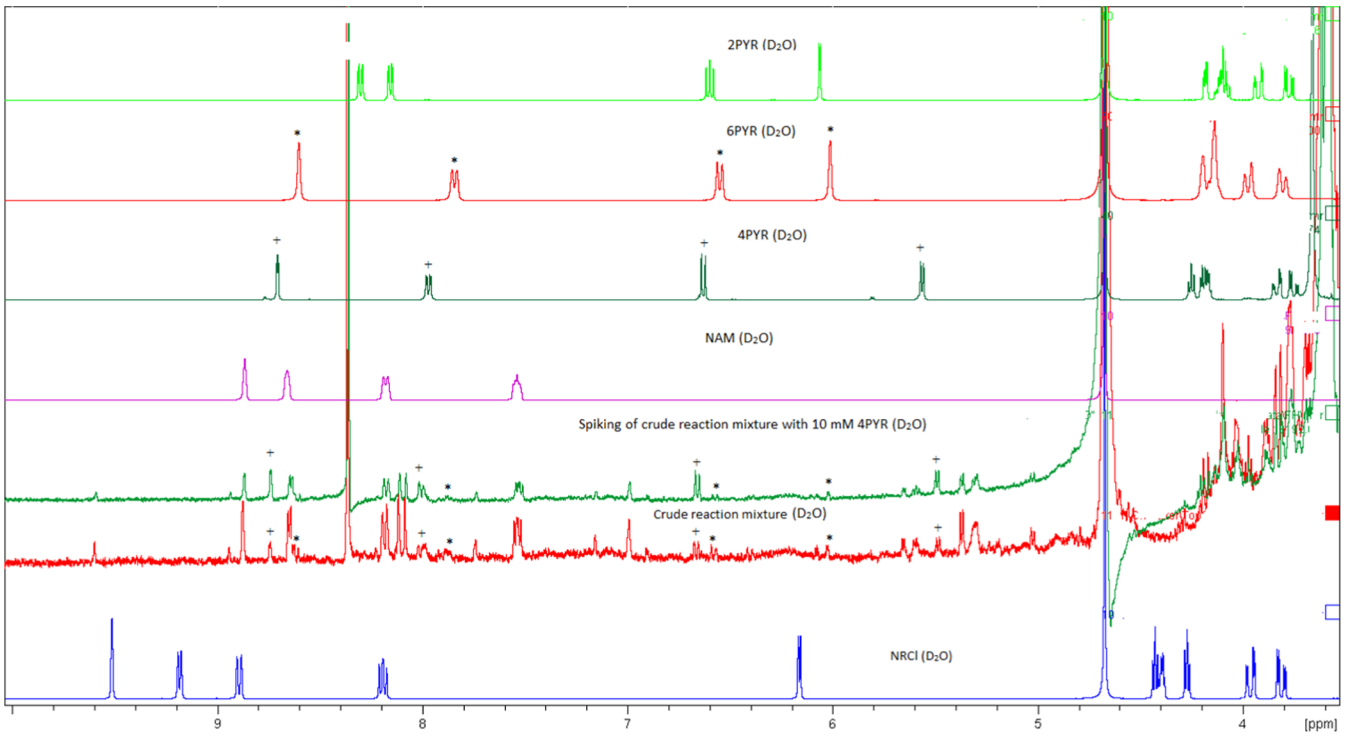

Figure 2. 4-PYR forms upon the reaction of NR^+ with superoxide. **Red**: ^1H NMR in D_2O of the reaction mixture of NR^+ with KO_2 in the presence of 18-crown-6 after 16 h at room temperature. **Green**: NMR sample spiked with authentic 4-PYR. ^1H NMR in D_2O of NRCl (blue), Nam (pink), 4-PYR (dark green), 6-PYR (red), and 2-PYR (fluorescent green).

NAD^+ and its phosphorylated form, NADP.[15,16] Chemical reactions employing reactive oxygen species generated by Fenton chemistry or metal-coupled redox chemistry oxidize nicotinamide riboside (NR^+) and NAD^+ at the 2 and 6 positions of the pyridinium ring.[7] As such, 2-PYR, 6-PYR (Figure 1), 2-ox-NAD, and 6-ox-NAD (Figure 1) are generated under alkaline ferricyanide conditions.[7] Oxidation of *N*-Me-Nam and nicotinamide mononucleotide (NMN) under these conditions leads to *N*-Me-2- and 6-PY and 2- and 6-PYR monophosphate,[7,15] respectively. However, all attempts to generate the 4-isomer under these conditions have failed.

Considering the abundance of the 4-PYR series in nature, another biochemical mechanism of formation must occur. Carrey proposed that 4-PYR originated from a MoCo-dependent aldehyde oxidase activity acting on nicotinamide riboside (NR^+)[11] in a mechanism reminiscent of *N*-Me-6-PY

https://doi.org/10.1021/acs.chemrestox.3c00264
Chem. Res. Toxicol. 2024, 37, 248−258

Scheme 1. Reaction of NR^+ with Superoxide in DMSO in the Presence of 18-Crown-6

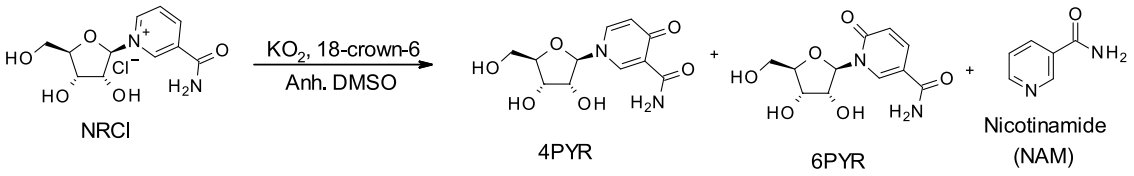

Scheme 2. General Approach to the Synthesis of 2, 4, and 6-Ox-NAD^+

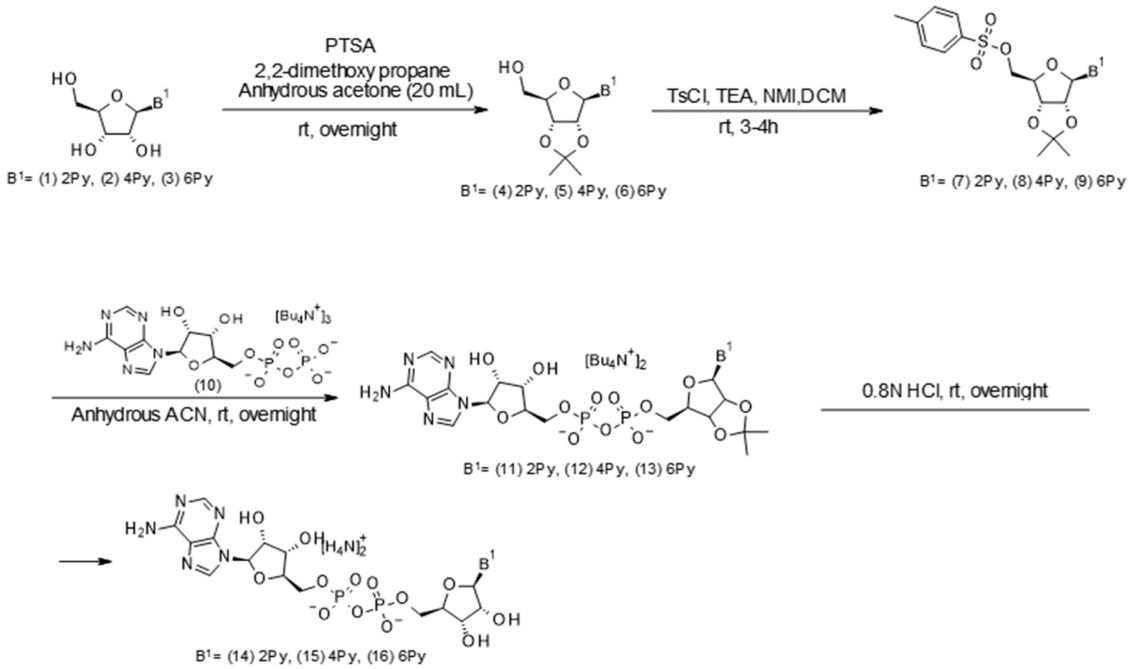

and *N*-Me-4-PY formation. However, while NR^+ is an endogenous NAD^+ precursor, circulating NR^+ has endogenous stability issues associated with glycohydrolase and phosphorylase activities (e.g., CD38-, BST1-, and PNP-catalyzed hydrolysis).[17] In 2015, Kammerer observed that 4-PYR and NR^+ levels in the extracellular media of different breast cancer cell lines did not directly correlate.[10] As such, circulating and intracellular NR^+ concentrations are low and unlikely to sustain 4-PYR formation.

Similarly, Slominka evaluated 4-PY as a putative substrate for phosphoribosyl transferases but observed no conversion.[13] Based on this report, we concluded that an alternative pathway to the noncanonical 4-PYR series must be at play. We and others observed that 4-PYR and 4-ox-NAD(P) forms under riboflavin-dependent redox processes,[16,18] as side reactions between superoxide[19] and the pyridinyl riboside moiety of NR^+ or $NAD(P)^+$ enabled by flavin-dependent enzymes, respectively. We also observed that an increased abundance of intracellular NADH increased the levels of ox-NAD in hepatocarcinoma HepG3 cells.[20] Yet, we could not confirm whether one isomer or multiple isomers of ox-NAD were responsible for this increase.

To address the need for better characterization of the oxidized catabolites of the NAD^+ metabolome, we first reported the synthesis of each isomer of the PYR series and the methylated PY series.[7] The PY, Me-PY, and PYR series can be separated by liquid chromatography. By having each one of the ribosylated pyridones at hand, we can now attempt to detect each isomer of the PY, Me-PY, and PYR series in urine and serum by liquid chromatography combined with mass spectrometry (LC-MS). Similarly, we needed synthetic standards for LC-MS analyses to measure ox-NAD species in cell cultures and cell-containing biospecimens. Here, we report the total synthesis and characterization of the three ox-NAD isomers and provide evidence that ox-NAD is detected in biological specimens. Furthermore, we demonstrate that all three isomers of ox-NAD are readily metabolized to their PYR parent molecule and, thus, are the likely precursors of the circulating and excreted PYRs. Finally, we evaluated whether the presence of ox-NAD could affect commonly used NAD assays that require redox chemistry to reveal NAD levels and observed that ox-NAD altered the measurements of NAD(H) concentration of standard solutions.

RESULTS

Reaction of NR^+ and NAD^+ with Superoxide Results in the Formation of 4-PYR and 4-ox-NAD. NRH/NAD(P)H and flavin-dependent enzymes and complexes can generate superoxide.[19,21] Under such circumstances, the resulting electrophilic superoxide is poised to react with the pyridinium of NR^+ or $NAD(P)^+$. We examined whether, in the absence of an enzyme as a catalyst, superoxide could react with the electron-deficient C-4 position of NR^+ to generate 4-PYR. Using potassium superoxide (KO_2, 4 equiv) and 18-crown-6 (1 equiv)[22] in anhydrous DMSO, 4-PYR formed as the major oxidation product (Figure 2). Along with 4-PYR, we also observed 6-PYR present in a lesser amount and substantial degradation of NR^+ to nicotinamide. While the chemical

https://doi.org/10.1021/acs.chemrestox.3c00264
Chem. Res. Toxicol. 2024, 37, 248−258

Scheme 3. Conversion of the Free Acid Form of Adenosine Diphosphate (ADP, 17) to the Tetrabutylammonium Salt form of ADP (10)

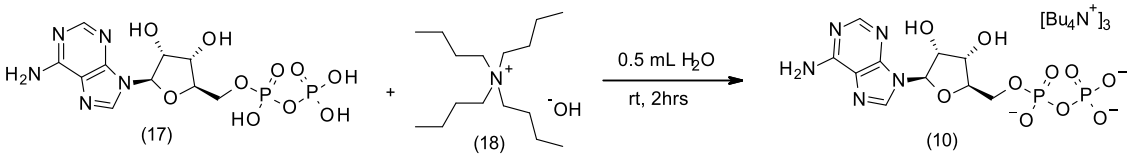

Table 1. Summary Table of the Mass Spectrometric Characteristics of the Me-Nam, Me-PY, PY, PYR, and ox-NAD

	isomers	ion formula	ionization	*m/z*	MS^2 fragments
Me-Nam		$C_7H_9N_2O$	M^+	137.0715	123.05584
Me-PY	Me-2-, 4-, 6-PY	$C_7H_9N_2O_2$	$M + H^+$	153.0664	139.05076 (weak)
PY	2-, 4-, 6-PY	$C_6H_7N_2O_2$	$M + H^+$	139.0507	N/A
PYR	2-, 4-, 6-PYR	$C_{11}H_{15}N_2O_6$	$M + H^+$	271.0924	139.05076
ox-NAD	2-, 4-, 6-ox-NAD	$C_{21}H_{28}N_7O_{15}P_2$	$M + H^+$	680.1113	139.05076, 136.06232

conversion is low yielding (~5−10%), it provides some evidence that just like Fenton chemistry, which generates hydroxide radical under basic conditions and results in the formation of the hydroxylated pyridinium riboside at the 2- and 6-position of the pyridinium ring, superoxide reacts with NR^+ to generate derivatives that are hydroxylated at the 4-position. It is, therefore, possible that superoxide generated by flavin-dependent enzymes, using both FMN/FAD and NRH or NAD(P)H for catalysis, facilitates the formation of 4-PYR and 4-ox-NAD(P), respectively, via its reaction with the electron-poor pyridinium ring of NR^+ and $NAD(P)^+$ (Scheme 1).

Synthetic Procedures. We recently reported the synthesis of each isomer of the pyridone riboside series (e.g., 2-PYR, 4-PYR, and 6-PYR).[7] We also reported the synthesis of 4-ox-NAD from 4-PYR-monophosphate enabled by mechanochemistry, whereby we sought a versatile approach to dinucleotide synthesis via pyrophosphate bond formation.[23] However, this chemistry is cumbersome as homodimers formed readily and required extensive purification for their removal. Therefore, we have developed a strategy for which the pyrophosphate linkage is preinstalled as an adenosine diphosphate. Nucleophilic displacement at the C5′-position of a suitably protected PYR allows access to the ox-NAD series without contamination with dimeric species. Scheme 2 describes the synthetic strategy to generate the ox-NAD series.

The starting materials, PYRs **1**−**3** (2-, 4-, and 6-PYR, respectively), were prepared according to our published procedure.[7] They were first converted to the 2′,3′-acetonide using 2,2-dimethoxypropane and para-toluenesulfonic acid (PTSA) in anhydrous acetone. The reaction was monitored by ^1H NMR analysis of the crude mixture in deuterated acetone. Upon completion, salts were filtered off, and PTSA was neutralized with aq. NH_4OH before removal of acetone under reduced pressure. The residue was purified by silica flash column chromatography on a Teledyne system, yielding protected nucleosides **4**−**6** in 77−88% yields. After purification, each isomer was converted to the corresponding tosylate **7**−**9** in 78−92% yields. All three tosylates (**7**−**9**) were hygroscopic and had to be stored in a desiccator over P_2O_5. The ox-NAD derivatives were then generated by nucleophilic displacement of the tosyl moiety by adenosine diphosphate (ADP). The poor solubility of the commercially available free acid form of ADP, $3H^+$-ADP, in acetonitrile was a limiting factor for this chemistry, as was its water content. Therefore, the dry tetrabutylammonium salt form of ADP was generated in-house. To convert the free acid of ADP to the tetrabutylammonium salt, the pH of $3H^+$-ADP (**17**) dissolved in water was adjusted to 7 by dropwise addition of conc. aq. $Bu_4N^+OH^-$. ^{31}P NMR showed a signal shift after forming the tetrabutylammonium salt form of ADP (**10**, Scheme 3). The resulting solution was lyophilized and subsequently azeotroped with toluene. The $(Bu_4N)_3$ADP water content was measured by ^1H NMR in d_4-MeOH.

The acetonide-protected pyridone adenine dinucleotide derivatives **11**−**13** (Scheme 2) were obtained by simply stirring the tosylates **7**−**9** with adenosine diphosphate tetrabutylammonium salt in anhydrous acetonitrile. The reaction was monitored by ^{31}P NMR, and upon completion of the reaction, acetonitrile was removed under reduced pressure, and the crude products were used in the next step without further purification. The fully deprotected pyridone adenine dinucleotides **14**−**16** were obtained upon deprotection of the acetonide using 0.8 M aq. HCl at room temperature. The purification was performed by C18 silica gel column chromatography using 100 mM ammonium acetate buffer (pH = 7) and acetonitrile mixtures (98:2 to 85:15%) as eluents to yield the three ox-NAD in 25−40% isolated yields measured by UV at 256 nm (adenosine absorbance). ^1H, ^{13}C, ^{31}P NMR, and HRMS analyses were performed to characterize each ox-NAD isomer.

Mass Spectrometry on the PY, *N*-Me-PY, PYR, and ox-NAD Series. All three isomers of PY, *N*-Me-PY, PYR, and ox-NAD have been examined for their mass spectrometric properties as pure samples (see SI for details, Figure S1A−D). The fragmentation pattern of the three isomers has been reported previously. Under high-energy ionization conditions,[7] a loss of ammonia has been observed for the 2 and the 4-isomers but not for the 6-isomer. However, these fragmentation patterns are more difficult to observe under milder ionization conditions. Here, the PY series does not fragment and the *N*-Me-PY series fragments to reveal a PY + H^+ ion, although less well than the pyridone ribosides, PYR, and the ox-NAD series. However, under the conditions that we have developed to examine the full NAD(P)(H) metabolome, the three isomers within each series sometimes share similar elution profiles (SI, Figure S1D). This is particularly noticeable for the PYR and ox-NAD series. This overlap is likely encountered by other research groups reporting on the oxidized forms of nicotinamide, methyl nicotinamide, NR^+, and NAD^+, thus accounting for the lack of comprehensive

https://doi.org/10.1021/acs.chemrestox.3c00264
Chem. Res. Toxicol. 2024, 37, 248−258

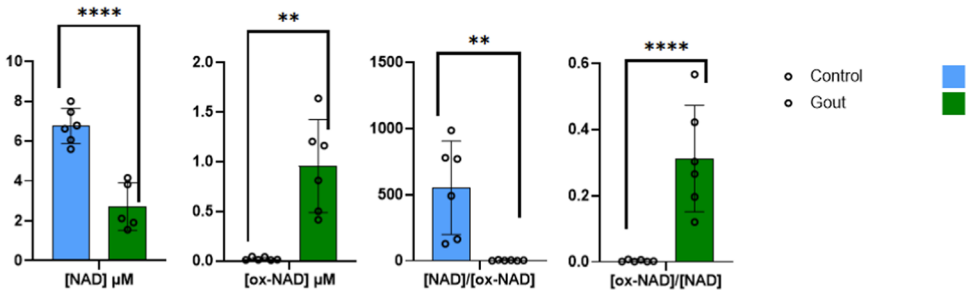

Figure 3. NAD^+ and ox-NAD levels in blood of healthy and gout patients. Concentrations in μM (left). Ratios of [NAD^+] to [ox-NAD] and vice versa are shown (right). Data normalized to the blood volume and spiked mass +3 NAD^+ as an internal standard. *$p < 0.05$, **$p < 0.01$, and ****$p < 0.0001$.

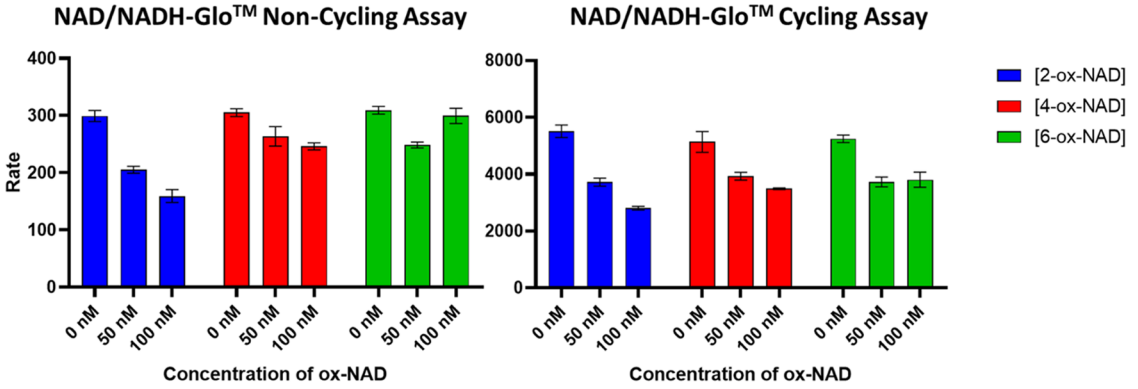

Figure 4. Effect of ox-NAD on the rates of detection using the Promega NAD/NADH-Glo assay. Since the actual [NAD(H)] concentrations are correlated to the rates using a standard curve, the measurements of [NAD(H)] are affected by the presence of ox-NAD in the standard cycling assay. Under noncycling assay, the 2-ox-NAD reduces the luciferase's ability to consume NADH.

description of the individual species in the literature.[5] We are currently developing series-specific separation methods to address this shortcoming of LC-MS detection and quantification. It should also be noted that nicotinamide guanine dinucleotide (NGD), an analogue of NAD^+, reported to be present in biological samples,[33] possesses the same m/z as ox-NAD. ox-NAD is differentiated from NGD by MS^2 analysis if the chemical standards are not available since NGD fragments to reveal 123 and 152 (Nam + H^+ and guanine + H^+) while ox-NAD fragments to 136 and 139 (adenine + H^+ and PY + H^+) (Table 1).

Detection of PYR and ox-NAD in Urine and Blood Transfusion Samples, Respectively. Reports of PY and Me-PY are inconsistent in publications where the NAD metabolome measurements are reported, and reports of PYR are often linked to RNA-derived nucleoside analyses.[10,24] In this context, the PYR isomers are often abbreviated PNCR for 1-ribosyl-3-carbamoyl-4-oxo-pyridine (4-PYR) and 1-ribosyl-5-carbamoyl-2-oxo-pyridine (6-PYR). PYR isomers can be found in plasma and serum, although they are mainly measured in urine. 4-PYR has been identified by many as a precursor to ox-NAD.[25] When 4-PYR is administered to animals or cells, it proves to be cytotoxic and metabolized to 4-ox-NAD.[8,26,27] 4-PYR is the isomer most routinely detected, although 6-PYR (M + H^+ m/z @271; rt ~17 min) has been reported. Unfortunately, we are not yet able to differentiate the contribution made by 4-PYR (M + H^+ m/z @271; rt ~17.2 min) and 6-PYR (M + H^+ m/z @271; rt ~16.7 min) as these species are not comprehensively separated under the LC profile applied to identify the various metabolites the NAD^+ metabolome encompasses. Therefore, likely the three PYR isomers are misassigned and often under-reported. Surprisingly, as we sought to detect the PYR series in human urine samples, we observed that while the 4/6-PYR isomers were the major PYR metabolites in most samples, on some occasions, the 2-PYR isomer (M + H^+ m/z @271; rt ~18.7 min) was the only detectable PYR metabolite in urine (Figure S2A).

Notwithstanding the detection challenges of the PY, Me-PY, and PYR series components, the detection and reporting of ox-NAD-derived species in biospecimens other than cell cultures[20] and erythrocytes[11,12] have been nonexistent. Yet, we detect ox-NAD in blood transfusion products when we measure NAD^+ and NADH content (Figure S2B - red blood cells; Figure S2C - whole blood; Figure S2D - platelets). As such, ox-NAD is present in red blood cells, whole blood, and platelets. The MS^2 fragments of ox-NAD show at 139 (PY + H^+) and 136 (adenine + H^+), further confirming the presence of ox-NAD in blood products. The 4-ox-NAD isomer was substantially more abundant than 2- and 6-ox-NAD, although we cannot discount that under some circumstances, the 2- and the 6-isomers coelute with the 4-ox-NAD.

Higher Levels of ox-NAD are Detected in the Blood of Gout Patients. When measuring the levels of NAD^+ and ox-NAD present in blood specimens of healthy nongout subjects (n = 6, mean age = 58), we observe that the concentration of ox-NAD averaged at 0.02 μM compared to that of NAD^+ at 6.76 μM, offering a ~500-fold molar excess of NAD^+ compared to ox-NAD (Figure 3). However, when measuring the levels of ox-NAD present in blood specimens of gout (n = 6, mean age = 56, mean serum uric acid = 7.6 mg/dl), the average concentration of ox-NAD rises to ~1 μM. This relative increase by ~50-fold is matched by a decrease in

https://doi.org/10.1021/acs.chemrestox.3c00264
Chem. Res. Toxicol. 2024, 37, 248−258

[NAD^+] to ~3 μM in the gout patients, yielding a molar ratio between [NAD^+] and [ox-NAD] of ~3 to 1. The 4-ox-NAD isomer was substantially more abundant than 2- and 6-ox-NAD, although as noted the 2- and the 6-isomer might coelute with the 4-ox-NAD.

Classical NAD(H) Measurement by NAD(H)-Glo Assay in the Presence of ox-NAD. Each ox-NAD isomer is a mimic of NAD(H).[28] One circumstance where the presence of ox-NAD might affect NAD(H) biochemistry is when NAD(H)-dependent redox enzymes are used to measure NAD(H) levels in biological samples, such as the Promega NAD/NADH-Glo assay used to measure NAD in cells and tissue extracts. The NAD/NADH-Glo assays use a two-enzyme system whereby a NAD to NADH cycling enzyme converts NAD to NADH, and a luciferase oxidizes NADH back to NAD while generating a luminescent product. Considering that ox-NAD can be present in extracts measured by the NAD/NADH-Glo assay, we examined whether ox-NAD affected this cycling assay. We observed that when we applied the recommended assay conditions ($0 < [NAD(H)] < 500$ nM), 2- and 4-ox-NAD affected the measurements substantially when present at nanomolar concentration matching that of NAD(H).

Furthermore, we examined if each ox-NAD isomer modulated the rates of the cycling enzyme or the luciferase. To achieve this, we measured luminescence solely from luciferase oxidation of NADH in the absence of a cycling substrate and under standard cycling conditions (Figure 4). We observed that all three isomers led to a decrease in the reaction rates in the cycling assay. Yet, only the 2 and 4 isomers decreased reaction rates linked to the luciferase activity, with the 2-isomer being the most effective at affecting the luciferase activity (noncycling assay conditions). The 4-ox-NAD acts primarily on the cycling redox enzyme (cycling assay conditions, technical triplicates). The presence of 2 and 4-ox-NAD isomers leads to the under-representation of the actual NAD(H) concentration when the NAD/NADH-Glo assay is applied to quantitate NAD(H).

Some of the 400 human enzymes that use NAD^+ or NADH as a cofactor might be inhibited by ox-NAD. An intracellular increased abundance of ox-NAD combined with a decreased availability of NAD^+ might affect the catalytic turnover of such enzymes. As these enzymes encounter more ox-NAD, the effect of ox-NAD on cellular metabolism and cellular homeostasis might become physiologically relevant.[8,14,26,29] Considering that endogenous ox-NAD might affect NAD(H) measurements when present, alternative methods to measure NAD(H) are necessary to validate assays conducted under NAD(H) redox chemistry catalyzed by redox enzymes.

Metabolism of ox-NAD by Liver Extract Using ^{1}H and ^{31}P NMR Spectroscopy. To examine whether PY and PYR are catabolites of ox-NAD, we considered that since ox-NAD isomers are mimics of NAD^+ and NADH, they could be metabolized by enzymes that degrade NAD^+ and NADH. However, like NADH and unlike NAD^+, ox-NAD isomers are stable to enzymes that cleave the glycosidic bond in NAD^+, such as CD38, sirtuins, and poly-ADP-ribosyl-transferases. Instead, we considered that the most likely degradation pathway would occur via the hydrolysis of the pyrophosphate linkage.[30] Since PYR and PY are found in urine, we assumed that ox-NAD could be hydrolyzed to these species by pyrophosphatases, phosphatases, and phosphorylases. Yet, to avoid any biochemical bias, we decided to use mouse liver extracts since this tissue is likely to contain the necessary NAD(H)-degrading enzymes.

When each isomer of ox-NAD was incubated individually with liver extract in PBS buffer, the hydrolysis of the pyrophosphate linkage was fast and could be monitored by ^{31}P NMR. We quickly observed the formation of the corresponding pyridone riboside (SI, Figure S3). While each of the ox-NAD isomers was readily consumed in the presence of the liver extract as detected by ^{1}H NMR, we did not observe the appearance of the pyridone nucleobases, PY. Crucially, the location of the carbonyl on the pyridone moiety did not affect the rates at which the ox-NAD degraded to the PYR.[28] However, over time, we observed that the signal to noise was lost, likely due to the precipitation of liver proteins binding to the pyridone metabolites. To ensure that the enzymes responsible for the formation of PY species were not simply absent from the liver extract, we checked whether 2-, 4-, and 6-PYR could be substrates of the purine nucleoside phosphorylase, PNP,[31] or of the pyrimidine nucleoside phosphorylase, UPP1.[32] While each enzyme was able to hydrolyze a known substrate, nicotinamide riboside for PNP and uridine for UPP1, none of the PYRs were observed to release PY upon treatment with these hydrolases under any reaction condition tested (SI, Figure S4). Therefore, neither ox-NAD nor PYR isomers are direct precursors to the pyridone nucleobases PY. The formation of the PY series found in biological specimens remains unknown.

DISCUSSION

$NAD(P)^+$ is reversibly reduced to NAD(P)H in a multitude of redox enzyme reactions involving oxidizable and reducible substrates (e.g., glycolysis, mitochondrial complex I, TCA cycle, amino acid metabolism, and urea cycle, and fatty acid synthesis). Transfer of the hydride enables these redox enzymatic conversions. While adenosine of NAD(P)(H) is central to enzyme binding and recognition, the pyridinyl riboside moiety of NAD^+ and its reduced form in NADH is where the action is. Electron-rich species like $HO^{\cdot}$ react at the most electrophilic positions of the pyridinyl ring in *ortho* and *para* positions to generate the 2- and the 6-isomers. Unlike Fenton chemistry ($HO^{\cdot}$), the hyperoxidation of NRH and NAD(P)H by enzymes containing riboflavin cofactors showed specificity for the 4-position. This type of chemistry is favored by processes whereby a hydride of NRH and NAD(P)H is transferred to the riboflavin cofactor (FAD or FMN) to generate the pyridinyl riboside moiety. In the presence of oxygen and the absence of an alternative co-oxidant, the electrons of the reduced riboflavins can transfer to oxygen, generating superoxide that reacts with the still bound NR^+ moiety. Rearrangement followed by hydrogen peroxide radical loss forms the 4-PYR series. Although partially speculative, we have demonstrated the feasibility of this mechanism, which offers a rationale for forming 4-PYR and 4-ox-NAD(P) under oxidative and reductive stress conditions. As with any phosphorylated species, ox-NAD is an intracellular entity, while PYR, its nucleoside parent, is found mainly outside the cellular environment, including urine. Overall, while the detection of 4-PYR can be routinely achieved, the detection and quantification of the oxidized species derived from the oxidation of nicotinamide ribosylated species, including ox-NAD species in biospecimens, have been mainly nonexistent. This work addresses this limitation and proposes a pathway to their formation and degradation. This is the first report on the

https://doi.org/10.1021/acs.chemrestox.3c00264
Chem. Res. Toxicol. 2024, 37, 248−258

formation and presence of endogenous ox-NAD in biospecimens. Crucially, we demonstrate that endogenous ox-NAD affects [NAD(H)] measurements when NAD(H)-dependent redox enzymatic processes are applied to quantify NAD(H) levels in cells and tissue extracts.

EXPERIMENTAL SECTION

All of the reagents and solvents were purchased from Sigma-Aldrich, AK Scientific, VWR, and Fisher Scientific, while most of the deuterated solvents, such as methanol-d_4, D_2O, $CDCl_3$, acetone-d_6, and DMSO-d_6, were purchased from Oakwood Chemicals. Anhydrous DCM and acetonitrile were obtained by distillation over calcium hydride, and acetone was dried over activated molecular sieves. TLC routinely confirmed the purity of the products on Merck KGaA plates (Kieselgel $60F_{254}$); the appropriate solvent systems were used, and spots were visualized under UV light and/or by acquiring ^{1}H NMR spectra. ^{1}H NMR (400.11 MHz), ^{13}C NMR (100.62 MHz), and ^{31}P NMR (161.96 MHz) spectra were recorded on a Bruker Ascend 400 MHz ultrashield spectrometer (Bruker Biospin) in acetone-d_6, DMSO-d_6, methanol-d_4, and D_2O at 298 K. TopSpin 3.2 (Bruker BioSpin) was used for all NMR spectral acquisition and preprocessing. The automation of sample submission was performed using ICON-NMR (Bruker BioSpin). Chemical shifts were expressed in parts per million (ppm) and coupling constants J in hertz (Hz). The following abbreviations are used to describe peak patterns when appropriate: s (single), d (doublet), dd (double doublet), t (triplet), and m (multiplet). HRMS spectra were obtained on an LTQ Orbitrap XL mass spectrometer (HESI source, positive polarity, capillary temperature 200 °C, source voltage 3.0 kV). An Eppendorf 5415R refrigerated centrifuge (F-45-24-11 rotor) was used in conjunction with the specific protocols described below to process the biological samples (urine, blood, and mice liver).

General Procedure for the Generation of the 4-PYR. To a solution of nicotinamide riboside chloride salt (NR^+Cl^-, 50 mg, 1 equiv) in 2 mL of anhydrous DMSO was added 18-crown-6 (1 equiv, 51.73 mg), followed by the addition of KO_2 (4 equiv, 55.45 mg), and the resulting mixture was stirred at rt overnight under nitrogen. The reaction progress was monitored by ^{1}H NMR analysis in D_2O.

General Synthetic Procedure for the Preparation of Acetonide-Protected Pyridone Ribosides (4−6). To a solution of pyridone ribosides **1**−**3** (0.4 g, 1.48 mmol) in anhydrous acetone (20 mL), 2,2-dimethoxypropane (0.9 mL, 7.4 mmol) and p-toluenesulfonic acid (PTSA) (0.255 g, 1.48 mmol) were added and stirred at room temperature overnight under a nitrogen gas environment. The reaction progress was monitored by ^{1}H NMR analysis of the crude reaction mixture in acetone-d_6. Upon completion, the reaction mixture was neutralized by adding ammonium hydroxide solution (27−30%) until we did not get pH 7. After complete neutralization, the reaction mixture was filtered, the filtrate was evaporated under vacuum, and the residue was purified by flash column chromatography (*n*-hexane/ethyl acetate = 50:50 to 10:90%) to give the compounds **4**−**6** as a colorless syrup in 77−88% yields.

General Synthetic Procedure for the Preparation of C-5 Tosylate Derivatives of Acetonide-Protected Pyridone Ribosides (7−9). A mixture of acetonide-protected pyridone ribosides 4−6 (0.333 g, 1.07 mmol), *p*-toluenesulfonyl chloride (TsCl) (0.244 g, 1.284 mmol), triethylamine (0.223 mL, 1.605 mmol), and *n*-methylimidazole (0.085 g, 1.07 mmol) in 5 mL of anhydrous DCM was stirred at rt under nitrogen for 3−4 h. The reaction progress was monitored by ^{1}H NMR analysis of the crude reaction mixture in acetone-d_6. Upon completion, the reaction mixture was concentrated under reduced pressure. The residue was redissolved in a minimum amount of DCM/methanol mixture (9:1), adsorbed on silica gel, and purified by flash column chromatography by using *n*-hexane/ethyl acetate (70:30 to 50:50%) as an eluent to afford **7**−**9** in 78−92% yields.

General Synthetic Procedure for the Preparation of Acetonide-Protected 2, 4, and 6-ox-NAD Derivatives (11−13). A mixture of C-5 tosylate pyridone ribosides 7−9 (0.108 g, 0.234 mmol) and adenosine diphosphate tetrabutylammonium salt (0.100 g, 0.234 mmol; Scheme 2) in 4 mL of anhydrous acetonitrile was stirred at rt under nitrogen for 24 h. The reaction progress was monitored by ^{1}H and ^{31}P NMR analyses of the crude reaction mixture (50 μL of crude plus 450 μL of DMSO-d_6, ns = 100). The resulting mixture was concentrated upon completion, and the crude products (**11**−**13**) were used directly for the next step without further purification.

General Synthetic Procedure for the Preparation of 2, 4, and 6-ox-NAD Derivatives (14−16). A solution of acetonide-protected ox-NAD derivatives **11**−**13** in 5 mL of HCl (0.8N) was stirred at room temperature (rt) for 24 h, and the reaction progress was monitored by ^{1}H and ^{31}P NMR analyses. After complete acetonide deprotection, the pH of the reaction mixture was adjusted up to 7 by adding ammonium hydroxide solution (27−30%) dropwise. Ten mL of EtOAc was added to the reaction mixture to remove the organic impurities. The mixture was stirred at rt for 30 min, and the organic layer was removed. The aqueous layer was then concentrated, and the crude was redissolved in a minimum amount of water and adsorbed on silica gel for the purification through C18 (reversed-phase) column by using 100 mM ammonium acetate buffer (pH = 7)/acetonitrile (98:2 to 90%:10%) with the flow rate of 5 mL/min/test tube to give resulting products 14−16 in 25−40% yields.

(4) 2-PYR-Acetonide. Yield 85%; ^{1}H NMR (400 MHz, D_2O), δ, ppm: 8.29 (dd, J = 2 and 2.04 Hz, 1H, H-6_{2py}), 8.02 (dd, J = 1.96 and 1.96 Hz, 1H, H-4_{2py}), 6.56 (t, J = 7.1 Hz, 1H, H-5_{2py}), 5.95 (d, J = 2.24 Hz, 1H, H-1_{ribose}), 4.84 (dd, J = 2.36 and 2.36 Hz, 1H, H-2_{ribose}), 4.76 (dd, J = 2.92 and 2.88 Hz, 1H, H-3_{ribose}), 4.44−4.41 (m, 1H, H-4_{ribose}), 3.78 and 3.66 (AB part of ABX system, 2H, J_{AB} = 12.44 Hz, J_{AX} = 3.51 HZ, J_{BX} = 5.56 Hz, $H_{5A\text{-}ribose}$ and $H_{5B\text{-}ribose}$), 1.52 (s, 3H, $-CH_3$), 1.30 (s, 3H, $-CH_3$); ^{13}C NMR (100 MHz, D_2O), δ, ppm: 167.83 ($CONH_2$), 161.87 (CO_{2py}), 145.20 ($C6_{2py}$), 138.50 ($C4_{2py}$), 119.21 ($C3_{2py}$), 114.32 [$(CH_3)_2$-C], 107.31 ($C5_{2py}$), 94.39 ($C1_{ribose}$), 87.31 ($C4_{ribose}$), 85.68 ($C2_{ribose}$), 80.43 ($C3_{ribose}$), 61.22 ($C5_{ribose}$), 25.97 (CH_3), 24.17 (CH_3); HRMS calcd for $C_{14}H_{19}N_2O_6$ $[M + H]^+$ 311.1243 found 311.1268.

(5) 4-PYR-Acetonide. Yield 77%; ^{1}H NMR (400 MHz, D_2O), δ, ppm: 8.64 (d, J = 2.38 Hz, 1H, H-2_{4py}), 7.99 (dd, J = 2.4 and 2.4 Hz, 1H, H-6_{4py}), 6.59 (d, J = 7.64 Hz, 1H, H-5_{4py}), 5.74 (d, J = 3.12 Hz, 1H, H-1_{ribose}), 4.93−4.87 (m, 2H, H-2 and H-3_{ribose}), 4.37 (q, J = 3.4 Hz, 1H, H-4_{ribose}), 3.78 and 3.72 (AB part of ABX system, 2H, J_{AB} = 12.56 Hz, J_{AX} = 3.28 HZ, J_{BX} = 4.2 Hz, $H_{5A\text{-}ribose}$ and $H_{5B\text{-}ribose}$), 1.53 (s, 3H, $-CH_3$), 1.30 (s, 3H, $-CH_3$); ^{13}C NMR (100 MHz, D_2O), δ, ppm: 178.97 (CO_{4py}), 167.63 ($CONH_2$), 142.76 ($C2_{2py}$), 138.72 ($C6_{4py}$), 120.36 ($C3_{4py}$), 118.15 ($C5_{4py}$), 115.46 [$(CH_3)_2$-C], 98.55 ($C1_{ribose}$), 86.23 ($C4_{ribose}$), 84.65 ($C2_{ribose}$), 80.41 ($C3_{ribose}$), 61.05 ($C5_{ribose}$), 25.96 (CH_3), 24.23 (CH_3); HRMS calcd for $C_{14}H_{19}N_2O_6$ $[M + H]^+$ 311.1243 found 311.1264.

(6) 6-PYR-Acetonide. Yield 88%; ^{1}H NMR (400 MHz, D_2O), δ, ppm: 8.39 (d, J = 2.52 Hz, 1H, H-2_{6py}), 7.83 (dd, J = 2.56 and 2.56 Hz, 1H, H-4_{6py}), 6.52 (d, J = 9.48 Hz, 1H, H-5_{6py}), 5.94 (d, J = 2.24 Hz, 1H, H-1_{ribose}), 4.88 (dd, J = 2.28 and 2.28 Hz, 1H, H-2_{ribose}), 4.78 (dd, J = 3.12 and 3.88 Hz, 1H, H-3_{ribose}), 4.43−4.40 (m, 1H, H-4_{ribose}), 3.80 and 3.66 (AB part of ABX system, 2H, J_{AB} = 12.4 Hz, J_{AX} = 3.56 HZ, J_{BX} = 5.72 Hz, $H_{5A\text{-}ribose}$ and $H_{5B\text{-}ribose}$), 1.52 (s, 3H, $-CH_3$), 1.29 (s, 3H, $-CH_3$); ^{13}C NMR (100 MHz, D_2O), δ, ppm: 168.92 ($CONH_2$), 163.69(CO_{6py}), 139.44 ($C2_{6py}$), 136.85 ($C4_{6py}$), 118.93 ($C3_{6py}$), 114.49 ($C5_{6py}$), 113.71 [$(CH_3)_2$-C], 94.22 ($C1_{ribose}$), 87.31 ($C4_{ribose}$), 85.39 ($C2_{ribose}$), 80.36 ($C3_{ribose}$), 61.17 ($C5_{ribose}$), 25.94 (CH_3), 24.19 (CH_3); HRMS calcd for $C_{14}H_{19}N_2O_6$ $[M + H]^+$ 311.1243 found 311.1267.

(7) 2-PYR-Acetonide Tosylate. Isolated yield 78%; ^{1}H NMR (400 MHz, D_2O), δ, ppm: 8.42 (dd, J = 2.04 and 2.04 Hz, 1H, H-6_{2py}), 7.84 (dd, J = 1.88 and 1.88 Hz, 1H, H-4_{2py}), 7.67 (d, J = 8.24 Hz, 2H Ar−H), 7.26 (d, J = 8.04 Hz, 2H, Ar−H), 6.48 (t, J = 6.98 Hz, 1H, H-5_{2py}), 5.85 (s, 1H, H-1_{ribose}), 5.00 (d, J = 5.4 Hz, 1H, H-2_{ribose}), 4.42−4.32 (m, 4H, H-3,4 and $5_{(AB)ribose}$), 2.36 (s, 3H, $-CH_3$), 1.51 (s, 3H, $-CH_3$), 1.30 (s, 3H, $-CH_3$); ^{13}C NMR (100 MHz, D_2O), δ, ppm: 166.06 ($CONH_2$), 161.30 (CO_{2py}), 145.25(Ar−C), 144.82($C6_{2py}$), 140.72 ($C4_{2py}$), 132.35 (Ar−C), 129.51 (Ar−C), 127.64 (Ar−C),

https://doi.org/10.1021/acs.chemrestox.3c00264
Chem. Res. Toxicol. 2024, 37, 248−258

120.88 ($C3_{2py}$), 113.77 [$(CH_3)_2$-C], 106.17 ($C5_{2py}$), 97.61 ($C1_{ribose}$), 86.51 ($C4_{ribose}$), 85.07 ($C2_{ribose}$), 81.40 ($C3_{ribose}$), 69.84 ($C5_{ribose}$), 25.97 (CH_3), 24.23 (CH_3), 20.35 (CH_3); HRMS calcd for $C_{21}H_{25}N_2O_8S$ $[M + H]^+$ 465.1332 found 465.1368.

(8) 4-PYR-Acetonide Tosylate. Isolated yield 84%; ^{1}H NMR (400 MHz, D_2O), δ, ppm: 8.58 (d, J = 2.3 Hz, 1H, H-2_{4py}), 7.81 (dd, J = 2.4 and 2.4 Hz, 1H, H-6_{4py}), 7.74 (d, J = 8.28 Hz, 2H Ar−H), 7.38 (d, J = 7.00 Hz, 2H, Ar−H), 6.53 (d, J = 7.64 Hz, 1H, H-5_{4py}), 5.73 (d, J = 3.0 Hz, 1H, H-1_{ribose}), 4.83 (s, 2H, H-2 and H-3_{ribose}), 4.51 (d, J = 3.0 Hz, 1H, H-4_{ribose}), 4.34−4.32 (m, 2H, $H_{5A\text{-}ribose}$ and $H_{5B\text{-}ribose}$), 2.42 (s, 3H, $-CH_3$), 1.53 (s, 3H, $-CH_3$), 1.30 (s, 3H, $-CH_3$); ^{13}C NMR (100 MHz, D_2O), δ, ppm: 178.34 (CO_{4py}) 166.46 ($CONH_2$), 145.61 (Ar−C), 142.20 ($C2_{4py}$), 137.32 ($C6_{4py}$), 132.28 (Ar−C), 129.77 (Ar−C), 127.65 (Ar−C), 120.88 ($C3_{4py}$), 118.43 ($C5_{4py}$), 114.94[$(CH_3)_2$-C], 98.68 ($C1_{ribose}$), 84.84 ($C4_{ribose}$), 83.72 ($C2_{ribose}$), 80.53 ($C3_{ribose}$), 68.78 ($C5_{ribose}$), 25.83 (CH_3), 23.93 (CH_3), 20.20 (CH_3); HRMS calcd for $C_{21}H_{25}N_2O_8S$ $[M + H]^+$ 465.1332 found 465.1363.

(9) 6-PYR-Acetonide Tosylate. Isolated yield 92%; ^{1}H NMR (400 MHz, D_2O), δ, ppm: 8.24 (s, 1H, H-2_{6py}), 7.83 (dd, J = 2.52 and 2.52 Hz, 1H, H-4_{6py}), 7.71 (d, J = 8.28 Hz, 2H Ar−H), 7.32 (d, J = 8.00 Hz, 2H, Ar−H), 6.44 (d, J = 9.52 Hz, 1H, H-5_{6py}), 5.82 (d, J = 1.2 Hz, 1H, H-1_{ribose}), 4.99 (dd, J = 1.4 and 1.44 Hz, 1H, H-2_{ribose}), 4.83−4.78 (m, 1H, H-3_{ribose}), 4.39−4.32 (m, 3H, H-4 and H-5AB$_{ribose}$), 2.39 (s, 3H, $-CH_3$), 1.52 (s, 3H, $-CH_3$), 1.31 (s, 3H, $-CH_3$); ^{13}C NMR (100 MHz, D_2O), δ, ppm: 166.95 ($CONH_2$), 162.32(CO_{6py}), 145.15 (Ar−C), 138.98 ($C2_{6py}$), 138.75 ($C4_{6py}$), 132.55 (Ar−C), 129.15 (Ar−C), 127.66 (Ar−C), 119.39 ($C3_{6py}$), 113.85 ($C5_{6py}$), 113.61 [$(CH_3)_2$-C], 97.06 ($C1_{ribose}$), 86.17 ($C4_{ribose}$), 84.92 ($C2_{ribose}$), 81.39 ($C3_{ribose}$), 69.85 ($C5_{ribose}$), 25.91 (CH_3), 23.94 (CH_3), 20.23 (CH_3); HRMS calcd for $C_{21}H_{25}N_2O_8S$ $[M + H]^+$ 465.1332 found 465.1361.

(14) 2-ox-NAD, NH_4^+ Salt. Isolated yield 25% measured by UV; ^{1}H NMR (400 MHz, D_2O), δ, ppm: 8.21 (s, 1H, H-$8_{adenine}$), 7.99 (s, 1H, H-$2_{adenine}$), 7.95 (dd, J = 2.04 and 2.0 Hz, 1H, H-6_{2py}), 7.89 (dd, J = 2.0, 2.04 Hz, 1H, H-4_{2py}), 6.35 (t, J = 7.14 Hz, 1H, H-5_{2py}), 5.90 (d, J = 2.24 Hz, 1H, H-$1_{AD\text{-}ribose}$), 5.87 (d, J = 5.48 Hz, 1H, H-$1_{2py\text{-}ribose}$), 4.52 (t, J = 5.28 Hz, 1H, H-$2_{AD\text{-}ribose}$), 4.35−4.01 [m, 9H (H-2, 2 × H-3, 2 × H-4 and 2 × H-5AB)$_{ribose}$]; ^{13}C NMR (100 MHz, D_2O), δ, ppm: 167.33 ($CONH_2$), 161.40 (CO-$C2_{2py}$), 155.16, 152.45, 148.82, 143.99, 139.81, 138.06, 118.15, 117.99, 107.62 (Ar−C), 91.17, 88.28, 84.21, 83.38, 77.03, 76.33 71.68, 69.67, 66.22, 65.00 [C1−5]ribose$_{(Adenosine\&2PY)}$; ^{31}P NMR (162 MHz, D_2O), δ, ppm: −10.90; HRMS calcd for $C_{21}H_{28}N_7O_{15}P_2$ $[M + H]^+$ 680.1113 found 680.1097.

(15) 4-ox-NAD, NH_4^+ Salt. The spectrometric analyses of **15** match those reported.[23]

(16) 6-ox-NAD, NH_4^+ Salt. Isolated yield 40%; ^{1}H NMR (400 MHz, D_2O), δ, ppm: 8.17 (s, 1H, H-$8_{adenine}$), 7.93 (s, 1H, H-2_{6PY}), 7.90 (s, 1H, H-2 $_{adenine}$), 7.56 (dd, J = 2.56 Hz, 2.56 Hz, 1H, H-4_{6py}), 6.27 (s, 1H, H-5_{6PY}), 5.75 (d, J = 5.4 Hz, 1H, H-$1_{AD\text{-}ribose}$), 5.69 (d, J = 3.16 Hz, 1H, H-$1_{6py\text{-}ribose}$), 4.45 (t, J = 5.36 Hz, 1H, H-$2_{AD\text{-}ribose}$), 4.29 (t, J = 5.36 Hz, 1H, H-$2_{6PY\text{-}ribose}$), 4.17−3.96 [m, 8H (2 × H-3, 2 × H-4 and 2 × H-5AB)$_{ribose}$]; ^{13}C NMR (100 MHz, D_2O), δ, ppm: 168.23 ($CONH_2$), 163.38 (CO-$C6_{6py}$), 155.24, 152.55, 148.62, 139.61, 139.37, 134.35, 118.60, 118.31, 114.11 (Ar−C), 89.77, 86.86, 83.31, 82.42, 74.98, 74.13, 69.93, 68.63, 65.28, 64.53 [C1−5]-ribose$_{(Adenosine\&6PY)}$; ^{31}P NMR (162 MHz, D_2O), δ, ppm: −11.10; HRMS calcd for $C_{21}H_{28}N_7O_{15}P_2$ $[M + H]^+$ 680.1113 found 680.1095.

Urine and Whole Blood Extraction Protocols. *Preparation of Biological Samples for Metabolic Analysis.* All of the samples were prepared using a liquid−liquid extraction process.

Urine. Sample Preparation (General Protocol). Collection and analyses of deidentified urine samples were approved by the University of South Alabama Institutional Biosafety Committee (IBC [1074523-6]). The following general protocol was applied for LC-MS sample preparation: A frozen (−80 °C) deidentified urine sample was held at room temperature for 30 min and then 2 mL of it was transferred to a 5 mL Eppendorf and frozen again at −80 °C. The complete frozen sample was then freeze-dried, and the solid residue was dissolved in a methanol (400 μL)−chloroform (400 μL) solution and vortexed three times. Sequentially, 200 μL of distilled water was added, then the mixture was vortexed again and kept at room temperature for 5 min. The sample was transferred to a clean 1.5 mL Eppendorf and centrifuged at 13,200 rpm (16,100 rcf) for 15 min at 4 °C to separate organic and aqueous layers. 400 μL of the top aqueous phase containing the metabolites was transferred to a clean 1.5 mL Eppendorf, carefully to avoid touching the organic phase with the pipet tip, and frozen at −80 °C for the lyophilization using a freeze-dryer. When drying, a small hole was made with the help of an injection needle into the lid of the closed Eppendorf tube to allow the solvent vapors to escape. After the freeze-drying process, the dried sample was stored at −80 °C (deep freezer) until analyzed by LC-MS. For the analysis of the sample by LC-MS, the dried material was dissolved in 20 μL of degassed buffer-A (10 mM ammonium acetate in 0.1% formic acid), centrifuged at 13,200 rpm (16,100 rcf) for 15 min at 4 °C, and then transferred to a mass vial for analysis.

Whole Blood. Sample Acquisition and General Sample Preparation Protocol. Collection and analyses of deidentified blood samples were approved by the University of South Alabama Institutional Biosafety Committee (IBC [1074523-6]). Nonfasting venous blood samples were collected into BD Vacutainer Venous Blood Collection Tubes containing spray-dried K2 EDTA. Deidentified samples were stored at −80 °C until thawed and aliquoted (100 μL) into 1.5 mL tubes. One aliquot was sent on dry ice to the USA metabolomics mass spectrometry core for LC-MS analysis. 400 μL of degassed MeOH was added directly to the 100 μL deidentified blood sample and sonicated at 4 °C three times (10 s each) to rupture the cell wall of blood cells, and then 400 μL of $CHCl_3$ and 200 μL of H_2O were subsequently added and vortexed. The sample was centrifuged at 13,200 rpm (16,100 rcf) for 15 min at 4 °C to separate organic and aqueous layers. 400 μL of the top aqueous phase containing the metabolites was transferred to a clean 1.5 mL Eppendorf, very carefully to avoid touching the organic phase with the pipet tip, and frozen at −80 °C for the lyophilization using a freeze-dryer. When drying, a small hole was made with the help of an injection needle into the lid of the closed Eppendorf tube to allow the solvent vapors to escape. After the freeze-drying process, the dried sample was stored at −80 °C (deep freezer) until we did not analyze it by MS. For the analysis of the sample by LC-MS, the dried material was dissolved in 20 μL of degassed buffer-A (10 mM ammonium acetate in 0.1% formic acid), centrifuged at 13,200 rpm (16,100 rcf) for 15 min at 4 °C, and then transferred to a mass vial for analysis.

LC-MS Procedure for Exact Mass and Biospecimen Analyses (Urine and Whole Blood). Six μL of dried sample dissolved in 20 μL of 10 mM ammonium acetate containing 0.1% formic acid was injected into the mass machine. LC separation was achieved on an Agilent 1200 series Liquid Chromatography (LC) with an Agilent Zorbax 300SB (C18, 2.1 mm × 150 mm) column. Initially, the flow rate was set at 50 μL per minute and ramped up to 150 μL/min in 20 min and held there until the run's end. Mobile phase A was 10 mM ammonium acetate in 0.1% formic acid (Fluke, NY), and mobile phase B was 0.1% formic acid in methanol (Thermo Fisher Scientific, Waltham, MA). Gradient conditions were 2% mobile phase B initially and raised to 95% in 20 min, held for 5 min, and brought it back to 2% in 15 min and finally equilibrated for 10 min. LC eluent was introduced to the Thermo Q Exactive Plus mass spectrometer (Thermo Scientific, San Jose, CA), equipped with electrospray ionization. The spray voltage and the capillary voltage were 3.2 kV and 320 °C, respectively. Data were acquired in positive ionization in SIM mode, and the acquired data were processed in Xcalibur. Two technical replicates were run for each biological repeat. The graph was plotted as the average of the peak values relative to their respective control ± SEM of at least two biological repeats.

NAD/NADH-Glo Cycling Enzyme Inhibition Assay. The concentration of nicotinamide adenine dinucleotide reduced form (NADH) in solution was assayed using the Promega NAD/NADH-Glo assay protocol in the presence and absence of ox-NAD. Stock solutions of β-nicotinamide adenine dinucleotide, reduced form disodium salt (Sigma-Aldrich), and ox-NAD were prepared fresh in 1 mM concentration. Each ox-NAD solution was diluted to a 2× concentration in phosphate-buffered saline (PBS) with [NADH]

https://doi.org/10.1021/acs.chemrestox.3c00264
Chem. Res. Toxicol. 2024, 37, 248−258

standardized at 400 nM. 25 μL samples of the respective solutions were incubated with 25 μL of the combined NAD/NADH-Glo detection reagent in a white 96-well luminometer plate. The luminescence was measured with the TECAN Infinite M1000 Pro microplate reader luminometer at 0, 10, and 20 min. Each point represents the average luminescence of triplicate reactions measured in relative light units (RLU).

NAD/NADH-Glo Luciferase Inhibition Assay. The concentration of nicotinamide adenine dinucleotide reduced form (NADH) in solution was assayed using the Promega NAD/NADH-Glo assay protocol in the presence and absence of ox-NAD with the exclusion of the NAD cycling enzyme from the detection mixture. Stock solutions of β-nicotinamide adenine dinucleotide, reduced form disodium salt (Sigma-Aldrich), and ox-NAD were prepared fresh in 1 mM concentration. Each ox-NAD solution was diluted to a 2× concentration in phosphate-buffered saline (PBS) with [NADH] standardized at 400 nM. 25 μL samples of the respective solutions were incubated with 25 μL of the combined NAD/NADH-Glo detection reagent without the NAD cycling enzyme added in a white 96-well luminometer plate. The luminescence was measured with the TECAN Infinite M1000 Pro microplate reader luminometer at 0, 10, and 20 min. Each point represents the average luminescence of triplicate reactions measured in relative light units (RLU).

Degradation of ox-NAD by Liver Enzymes. *Enzyme Activity Assay.* The hydrolysis of the pyrophosphate bond of 2-, 4-, and 6-ox-NAD by the enzymes present in the frozen mouse liver extract was performed in 50 mM HEPES buffer, containing 125 mM NaCl, 100 mM $MgCl_2$, 0.5 mg BSA per mL, FAD (5 μM per 20 mL of buffer), and 16% D_2O at 25 °C and was monitored by ^1H and ^{31}P NMR analysis. Incubations were conducted in the NMR tube, which contained a final volume of 600:400 μL of HEPES buffer (50.0 mM, pH 7.0, containing NaCl, $MgCl_2$, BSA, FAD), 100.0 μL of ox-NAD (1 mg per 100 μL D_2O, 15 mM), and 100 μL of fresh mouse liver extract. Measurements were taken at t = 0, 20, 30, 50, 60, and 70 min by ^1H (ns = 8) and ^{31}P NMR analysis (ns = 50). For each independent experiment, freshly prepared solutions of individual ox-NAD in 100 μL of D_2O were used.

Preparation of Fresh Mice Liver Extract. 400 mg of frozen mouse liver was beaten with small ceramic balls in a 2 mL plastic tube in the presence of 0.5 mL of HEPES buffer for 30 s. This process was repeated three times. Upon completion, the sample vial was centrifuged at 1000 rpm (100 rcf) for 5 min, and the supernatant was transferred to a 1.5 mL Eppendorf and cooled to 0 °C for 10 min. After 10 min, the supernatant was further centrifuged at 10,000 rpm (9300 rcf) for 10 min, and the mostly clear solution was transferred into a fresh 1.5 mL Eppendorf. The liver extract was stored on ice at 0 °C.

Effect of UPP1 and PNP Enzymes on 2-, 4-, and 6-PYR. *Enzyme Activity Assay.* Phosphorolysis of 2-, 4-, and 6-PYRs by the UPP1/PNP enzyme (uridine phosphorylase 1 human recombinant, ProSpec-Tany TechnoGene Ltd., and purine nucleoside phosphorylase, Sigma-Aldrich) was performed individually in HEPES buffer containing KH_2PO_4 at 25 °C and was monitored by ^1H NMR. Incubations were conducted in the NMR tube, which contained a final volume of 510:400 μL of HEPES buffer (100.0 mM, pH 7.0), 100.0 μL of PYRs (10.0 mM in 1 mL D_2O), and 10 μL of UPP1 (10 μg dissolved in 50 μL of HEPES buffer). Measurements were taken at t = 0, 1, 6, 12, and 24 h (ns = 128). To ensure the active nature of the enzyme, the same experiment was also performed with uridine.

Stability Study of 2-, 4-, and 6-PYR in Acidic and Basic Media. To check the stability of 2-, 4-, and 6-PYR in acid and basic media, 50 mM stock solutions of each pyridone riboside were prepared in 500 μL of D_2O. 50 μL of each 50 mM PYR D_2O stock solution was mixed with 450 μL of 1 N HCl or NaOH in an NMR tube, respectively. ^1H NMR analyzed the resulting mixtures, and the measurements were taken at t = 5 min, 12, 24, 48, 96, and 120 h (ns = 50−100).

CONCLUSIONS

The field of nicotinamide metabolism and NAD(P) over-oxidation has been plagued with unintentional structural misassignments, misleading nomenclature, and limited quantifications. Considering the structural similarity between ox-NAD and NAD(H), one can envisage that ox-NAD could compete with NAD(H) for NAD-dependent enzyme-binding sites and thus interfere with their ability to catalyze central metabolism. Measuring circulating PYR and ox-NAD is the first step toward determining whether the PYR and ox-NAD series are potentially detrimental endogenous metabolites. It is proposed that these issues are due to a lack of synthetic standards for LC-MS and $LC\text{-}MS^2$ analyses. Having synthesized and fully characterized each isomer of PY, Me-PY, PYR, and ox-NAD, we can now readily detect the different isomers of PYR in biospecimens. Although our conditions are not yet optimized for the specific separation of the ox-NAD isomers. Here, we have described the synthesis of each of the ox-NAD isomers and characterized the LC-MS profiles of the PYR series while providing protocols that allow for their detection in biospecimen extracts. Finally, we provide supporting evidence that oxidation of NAD(H) to ox-NAD offers the platform for forming the PYR isomers and that the PYR species are stable in solution containing liver enzymes, at least in vitro. Crucially, we demonstrate that ox-NAD can affect the in vitro NAD(H) level measurements conducted via chemoenzymatic assays on cells and tissue extracts.

ASSOCIATED CONTENT

Supporting Information

The Supporting Information is available free of charge at https://pubs.acs.org/doi/10.1021/acs.chemrestox.3c00264.

^1H and ^{13}C NMR chemical shift for the synthesized compounds (4−9, 14−16); description of biospecimens; LC-MS of the PY series and exact mass M + H^+@139; LC-MS of the ox-NAD series; effect of UPP1 enzyme on 2-, 4-, and 6-PYRs and uridine (^1H NMR, t = 0 24 h); and stability study of 2-, 4-, and 6-PYR in acidic and basic mediums (PDF)

AUTHOR INFORMATION

Corresponding Author

Marie E. Migaud − *Mitchell Cancer Institute, Frederick P. Whiddon College of Medicine, Department of Pharmacology, University of South Alabama, Mobile, Alabama 36604, United States;* orcid.org/0000-0002-9626-2405; Email: mmigaud@southalabama.edu

Authors

Faisal Hayat − *Mitchell Cancer Institute, Frederick P. Whiddon College of Medicine, Department of Pharmacology, University of South Alabama, Mobile, Alabama 36604, United States*

J. Trey Deason − *Mitchell Cancer Institute, Frederick P. Whiddon College of Medicine, Department of Pharmacology, University of South Alabama, Mobile, Alabama 36604, United States*

Ru Liu Bryan − *School of Medicine, University of California, San Diego, La Jolla, California 92093, United States; VA San Diego Healthcare System, San Diego, California 92161, United States*

Robert Terkeltaub − *School of Medicine, University of California, San Diego, La Jolla, California 92093, United States; VA San Diego Healthcare System, San Diego, California 92161, United States*

Weidan Song − *Cecil H. and Ida Green Center for Reproductive Biology Sciences, University of Texas Southwestern Medical Center, Dallas, Texas 75390, United States*

W. Lee Kraus − *Cecil H. and Ida Green Center for Reproductive Biology Sciences, University of Texas Southwestern Medical Center, Dallas, Texas 75390, United States;* orcid.org/0000-0002-8786-2986

Janice Pluth − *Department of Health Physics and Diagnostic Sciences, University of Nevada, Las Vegas, Las Vegas, Nevada 89154, United States*

Natalie R. Gassman − *Department of Pharmacology and Toxicology, Heersink School of Medicine, University of Alabama, Birmingham, Birmingham, Alabama 35294, United States;* orcid.org/0000-0002-8488-2332

Complete contact information is available at: https://pubs.acs.org/10.1021/acs.chemrestox.3c00264

Author Contributions

Conceptualization, M.E.M.; methodology, M.E.M., F.H., J.T.D., W.L.K.; formal analysis, M.E.M., F.H., J.T.D.; investigation, F.H., J.T.D., W.S.; resources, M.E.M., N.R.G, J.P., R.L.B.; data curation, M.E.M., R.L.B.; writing—original draft preparation, F.H.; writing—review and editing, M.E.M., N.R.G., J.P., R.L.B.; visualization, M.E.M., F.H., J.T.D.; supervision, M.E.M.; project administration, M.E.M.; funding acquisition, M.E.M., N.R.G, J.P. All authors have read and agreed to the published version of the manuscript. CRediT: **Jonathan Trey Deason** investigation, methodology; **Weidan Song** investigation.

Funding

This work (Project #T0702) is supported by the Translational Research Institute for Space Health through NASA Cooperative Agreement NNX16AO69A.

Notes

The authors declare no competing financial interest.

Ethics Animal tissue acquisition: This study was performed in strict accordance with the recommendations in the Guide for the Care and Use of Laboratory Animals of the National Institutes of Health. No animals were exclusively used for the purpose of this study. Instead, excess and unused tissue from control/untreated animals that had been euthanized under unrelated studies were used for this study. Liver tissues flash frozen in liquid nitrogen/stored at −80 °C generated according to protocols approved by the institutional animal care and use committee of the University of South Alabama were provided by Dr. Wito Richter (IACUC protocols #1567276 and #1644170). Human biospecimens acquisition: No biospecimens were collected and used exclusively for the purpose of this study. Instead, these samples were discarded, anonymized urine and blood samples, obtained according to protocols approved by the Institutional Biological Committee of the University of South Alabama (IBC protocol # 1074523-6).

■ ACKNOWLEDGMENTS

Data reported in this publication were obtained using the University of South Alabama Mass Spectrometry Facility, a core research resource supported by the Mitchell Cancer Center and the Frederick P. Whiddon College of Medicine at USA. Dr J. Clark and Dr L. Belfleur are thanked for their technical help in acquiring the MS data and developing the LC-MS method applied in this work. Finally, the authors thank Dr Wito Reichert, University of South Alabama, for providing the mice liver extracts.

■ REFERENCES

(1) Nikiforov, A.; Kulikova, V.; Ziegler, M. The human NAD metabolome: Functions, metabolism and compartmentalization. *Crit. Rev. Biochem. Mol. Biol.* **2015**, *50* (4), 284−297.

(2) (a) Berger, F.; Ramirez-Hernandez, M. H.; Ziegler, M. The new life of a centenarian: signalling functions of NAD(P). *Trends Biochem. Sci.* **2004**, *29* (3), 111−118. (b) Chu, X.; Raju, R. P. Regulation of NAD(+) metabolism in aging and disease. *Metabolism* **2022**, *126*, No. 154923.

(3) (a) Shibata, K.; Kawada, T.; Iwai, K. Simultaneous micro-determination of nicotinamide and its major metabolites, N1-methyl-2-pyridone-5-carboxamide and N1-methyl-4-pyridone-3-carboxamide, by high-performance liquid chromatography. *J. Chromatogr.* **1988**, *424* (1), 23−28. (b) Shibata, K.; Matsuo, H. Correlation between niacin equivalent intake and urinary excretion of its metabolites, N'-methylnicotinamide, N'-methyl-2-pyridone-5-carboxamide, and N'-methyl-4-pyridone-3-carboxamide, in humans consuming a self-selected food. *Am. J. Clin. Nutr.* **1989**, *50* (1), 114−119.

(4) Bhasin, S.; Seals, D.; Migaud, M.; Musi, N.; Baur, J. A. Nicotinamide Adenine Dinucleotide in Aging Biology: Potential Applications and Many Unknowns. *Endocr. Rev.* **2023**, *44*, 1047−1073, DOI: 10.1210/endrev/bnad019.

(5) Dhuguru, J.; Dellinger, R. W.; Migaud, M. E. Defining NAD(P)(H) Catabolism. *Nutrients* **2023**, *15* (13), No. 3064, DOI: 10.3390/nu15133064.

(6) (a) Mills, G. C.; Davis, N. J.; Lertratanangkoon, K. Isolation and Identification of 1-Ribosyl Pyridone Nucleosides from Human Urine. *Nucleosides and Nucleotides* **1989**, *8* (3), 415−430. (b) Intrieri, M.; Calcagno, G.; Oriani, G.; Pane, F.; Zarrilli, F.; Cataldo, P. T.; Foggia, M.; Piazza, M.; Salvatore, F.; Sacchetti, L. Pseudouridine and 1-ribosylpyridin-4-one-3-carboxamide (PCNR) serum concentrations in human immunodeficiency virus type 1-infected patients are independent predictors for AIDS progression. *J. Infect. Dis* **1996**, *174* (1), 199−203.

(7) Hayat, F.; Sonavane, M.; Makarov, M. V.; Trammell, S. A. J.; McPherson, P.; Gassman, N. R.; Migaud, M. E. The Biochemical Pathways of Nicotinamide-Derived Pyridones. *Int. J. Mol. Sci.* **2021**, *22* (3), No. 1145, DOI: 10.3390/ijms22031145.

(8) Mierzejewska, P.; Kunc, M.; Zabielska-Kaczorowska, M. A.; Kutryb-Zajac, B.; Pelikant-Malecka, I.; Braczko, A.; Jablonska, P.; Romaszko, P.; Koszalka, P.; Szade, J.; et al. An unusual nicotinamide derivative, 4-pyridone-3-carboxamide ribonucleoside (4PYR), is a novel endothelial toxin and oncometabolite. *Exp. Mol. Med.* **2021**, *53* (9), 1402−1412.

(9) (a) Dutta, S. P.; Crain, P. F.; McCloskey, J. A.; Chheda, G. B. Isolation and characterization of 1-β-D-ribofuranosylpyridin-4-one-3-carboxamide from human urine. *Life Sci.* **1979**, *24* (15), 1381−1388. (b) Mrochek, J. E.; Jolley, R. L.; Young, D. S.; Turner, W. J. Metabolic response of humans to ingestion of nicotinic acid and nicotinamide. *Clin. Chem.* **1976**, *22* (11), 1821−1827.

(10) Willmann, L.; Erbes, T.; Krieger, S.; Trafkowski, J.; Rodamer, M.; Kammerer, B. Metabolome analysis via comprehensive two-dimensional liquid chromatography: identification of modified nucleosides from RNA metabolism. *Anal. Bioanal. Chem.* **2015**, *407* (13), 3555−3566.

(11) Carrey, E. A.; Smolenski, R. T.; Edbury, S. M.; Laurence, A.; Marinaki, A. M.; Duley, J. A.; Zhu, L.; Goldsmith, D. J.; Simmonds, H. A. Origin and characteristics of an unusual pyridine nucleotide accumulating in erythrocytes: positive correlation with degree of renal failure. *Clin. Chim. Acta* **2003**, *335* (1−2), 117−129.

(12) (a) Carrey, E. A.; Smolenski, R. T.; Edbury, S. M.; Laurence, A.; Marinaki, A. M.; Duley, J. A.; Zhu, L. M.; Goldsmith, D. J.; Simmonds, H. A. An unusual pyridine nucleotide accumulating in erythrocytes: its identity and positive correlation with degree of renal failure. *Nucleosides, Nucleotides Nucleic Acids* **2004**, *23* (8−9), 1135−1139. (b) Laurence, A.; Edbury, S. M.; Marinaki, A. M.; Smolenski, R. T.; Goldsmith, D. J. A.; Simmonds, H. A.; Carrey, E. A. 4-pyridone-3-carboxamide ribonucleoside triphosphate accumulating in erythrocytes in end stage renal failure originates from tryptophan metabolism. *Clin. Exp. Med.* **2007**, *7* (4), 135−141. (c) Synesiou, E.; Fairbanks, L. D.; Simmonds, H. A.; Slominska, E. M.; Smolenski, R. T.; Carrey, E. A. 4-Pyridone-3-carboxamide-1-beta-D-ribonucleoside triphosphate (4PyTP), a novel NAD metabolite accumulating in erythrocytes of uremic children: a biomarker for a toxic NAD analogue in other tissues? *Toxins* **2011**, *3* (6), 520−537. (d) Shibata, K.; Fukuwatari, T. Pyridone compounds, catabolites of NAD are new uremic toxins. *Bitamin* **2007**, *81* (11), 571−574.

(13) Slominska, E. M.; Orlewska, C.; Yuen, A.; Osman, L.; Romaszko, P.; Sokolowska, E.; Foks, H.; Simmonds, H. A.; Yacoub, M. H.; Smolenski, R. T. Metabolism of 4-pyridone-3-carboxamide-1-beta-D-ribonucleoside triphosphate and its nucleoside precursor in the erythrocytes. *Nucleosides, Nucleotides Nucleic Acids* **2008**, *27* (6), 830−834.

(14) Rutkowski, B.; Rutkowski, P.; Slominska, E.; Smolenski, R. T.; Swierczynski, J. Cellular toxicity of nicotinamide metabolites. *J. Renal Nutr.* **2012**, *22* (1), 95−97.

(15) Brumaghim, J. L.; Li, Y.; Henle, E.; Linn, S. Effects of hydrogen peroxide upon nicotinamide nucleotide metabolism in Escherichia coli: changes in enzyme levels and nicotinamide nucleotide pools and studies of the oxidation of NAD(P)H by Fe(III). *J. Biol. Chem.* **2003**, *278* (43), 42495−42504.

(16) de Rosa, M.; Pennati, A.; Pandini, V.; Monzani, E.; Zanetti, G.; Aliverti, A. Enzymatic oxidation of NADP + to its 4-oxo derivative is a side-reaction displayed only by the adrenodoxin reductase type of ferredoxin-NADP + reductases. *FEBS J.* **2007**, *274* (15), 3998−4007.

(17) McReynolds, M. R.; Chellappa, K.; Chiles, E.; Jankowski, C.; Shen, Y.; Chen, L.; Descamps, H. C.; Mukherjee, S.; Bhat, Y. R.; Lingala, S. R.; et al. NAD(+) flux is maintained in aged mice despite lower tissue concentrations. *Cell Syst.* **2021**, *12* (12), 1160−1172.

(18) (a) Bossi, R. T.; Aliverti, A.; Raimondi, D.; Fischer, F.; Zanetti, G.; Ferrari, D.; Tahallah, N.; Maier, C. S.; Heck, A. J.; Rizzi, M.; Mattevi, A. A covalent modification of NADP + revealed by the atomic resolution structure of FprA, a Mycobacterium tuberculosis oxidoreductase. *Biochemistry* **2002**, *41* (28), 8807−8818. (b) Makarov, M. V.; Hayat, F.; Graves, B.; Sonavane, M.; Salter, E. A.; Wierzbicki, A.; Gassman, N. R.; Migaud, M. E. Chemical and Biochemical Reactivity of the Reduced Forms of Nicotinamide Riboside. *ACS Chem. Biol.* **2021**, *16* (4), 604−614.

(19) Miettinen, T. P.; Björklund, M. NQO2 Is a Reactive Oxygen Species Generating Off-Target for Acetaminophen. *Mol. Pharmaceutics* **2014**, *11* (12), 4395−4404.

(20) Sonavane, M.; Hayat, F.; Makarov, M.; Migaud, M. E.; Gassman, N. R. Dihydronicotinamide riboside promotes cell-specific cytotoxicity by tipping the balance between metabolic regulation and oxidative stress. *PLoS One* **2020**, *15* (11), No. e0242174.

(21) Grivennikova, V. G.; Vinogradov, A. D. Generation of superoxide by the mitochondrial Complex I. *Biochim. Biophys. Acta, Bioenerg.* **2006**, *1757* (5−6), 553−561.

(22) Jiang, W.; Zhang, X.; Sui, Z. Potassium superoxide as an alternative reagent for Winterfeldt oxidation of beta-carbolines. *Org. Lett.* **2003**, *5* (1), 43−46.

(23) Hayat, F.; Makarov, M. V.; Belfleur, L.; Migaud, M. E. Synthesis of Mixed Dinucleotides by Mechanochemistry. *Molecules* **2022**, *27* (10), No. 3229, DOI: 10.3390/molecules27103229.

(24) (a) Slominska, E. M.; Carrey, E. A.; Foks, H.; Orlewska, C.; Wieczerzak, E.; Sowinski, P.; Yacoub, M. H.; Marinaki, A. M.; Simmonds, H. A.; Smolenski, R. T. A novel nucleotide found in human erythrocytes, 4-pyridone-3-carboxamide-1-beta-D-ribonucleoside triphosphate. *J. Biol. Chem.* **2006**, *281* (43), 32057−32064. (b) Xu, G.; Schmid, H. R.; Lu, X.; Liebich, H. M.; Lu, P. Excretion pattern investigation of urinary normal and modified nucleosides of breast cancer patients by RP-HPLC and factor analysis method. *Biomed. Chromatogr.* **2000**, *14* (7), 459−463. (c) Henneges, C.; Bullinger, D.; Fux, R.; Friese, N.; Seeger, H.; Neubauer, H.; Laufer, S.; Gleiter, C. H.; Schwab, M.; Zell, A.; Kammerer, B. Prediction of breast cancer by profiling of urinary RNA metabolites using Support Vector Machine-based feature selection. *BMC Cancer* **2009**, *9*, No. 104, DOI: 10.1186/1471-2407-9-104.

(25) (a) Romaszko, P.; Slominska, E. M.; Orlewska, C.; Lipinski, M.; Smolenski, R. T. Metabolism of 4-pyridone-3-carboxamide-1-beta-D-ribonucleoside (4PYR) in rodent tissues and in vivo. *Mol. Cell. Biochem.* **2011**, *351* (1−2), 143−148. (b) Pelikant-Malecka, I.; Kaniewska-Bednarczuk, E.; Szrok, S.; Sielicka, A.; Sledzinski, M.; Orlewska, C.; Smolenski, R. T.; Slominska, E. M. Metabolic pathway of 4-pyridone-3-carboxamide-1beta-d-ribonucleoside and its effects on cellular energetics. *Int. J. Biochem. Cell Biol.* **2017**, *88*, 31−43. (c) Pelikant-Malecka, I.; Smolenski, R. T.; Slominska, E. M. Metabolism of 4-pyridone-3-carboxamide-1beta-d-ribonucleoside (4PYR) in primary murine brain microvascular endothelial cells (mBMECs). *Nucleosides, Nucleotides Nucleic Acids* **2018**, *37* (11), 639−644.

(26) (a) Koszalka, P.; Kutryb-Zajac, B.; Mierzejewska, P.; Tomczyk, M.; Wietrzyk, J.; Serafin, P. K.; Smolenski, R. T.; Slominska, E. M. 4-Pyridone-3-carboxamide-1-beta-D-ribonucleoside (4PYR)-A Novel Oncometabolite Modulating Cancer-Endothelial Interactions in Breast Cancer Metastasis. *Int. J. Mol. Sci.* **2022**, *23* (10), No. 5774, DOI: 10.3390/ijms23105774. (b) Slominska, E. M.; Borkowski, T.; Rybakowska, I.; Abramowicz-Glinka, M.; Orlewska, C.; Smolenski, R. T. In vitro and cellular effects of 4-pyridone-3-carboxamide riboside on enzymes of nucleotide metabolism. *Nucleosides, Nucleotides Nucleic Acids* **2014**, *33* (4−6), 353−357.

(27) (a) Zabielska, M.; Kutryb-Zajac, B.; Zukowska, P.; Slominska, E.; Smolenski, R. Effects of 4-Pyridone-3-carboxamide-1beta-D-ribonucleoside on adenine nucleotide catabolism in the aortic wall; Implications for atherosclerosis in ApoE−/−LDLR−/− mice. *Nucleosides, Nucleotides Nucleic Acids* **2016**, *35* (10−12), 720−725. (b) Pelikant-Malecka, I.; Sielicka, A.; Kaniewska, E.; Smolenski, R. T.; Slominska, E. M. Endothelial toxicity of unusual nucleotide metabolites. *Pharmacol. Rep.* **2015**, *67* (4), 818−822. (c) Romaszko, P.; Slominska, E. M.; Smolenski, R. T. Effect of 4-pyridone-3-carboxamide ribonucleoside (4PYR)-potential cardiovascular toxin in perfused rat heart. *Nucleosides, Nucleotides Nucleic Acids* **2014**, *33* (4−6), 333−337.

(28) Buckley, D. P.; Migaud, M. E.; Tanner, J. J. Conformational Preferences of Pyridone Adenine Dinucleotides from Molecular Dynamics Simulations. *Int. J. Mol. Sci.* **2022**, *23* (19), No. 11866, DOI: 10.3390/ijms231911866.

(29) Pelikant-Malecka, I.; Sielicka, A.; Kaniewska, E.; Smolenski, R. T.; Slominska, E. M. 4-Pyridone-3-carboxamide-1beta-D-ribonucleoside metabolism in endothelial cells and its impact on cellular energetic balance. *Nucleosides, Nucleotides Nucleic Acids* **2014**, *33* (4−6), 338−341.

(30) Kulikova, V. A.; Nikiforov, A. A. Role of NUDIX Hydrolases in NAD and ADP-Ribose Metabolism in Mammals. *Biochemistry* **2020**, *85* (8), 883−894.

(31) Hayat, F.; Migaud, M. E. Nicotinamide riboside-amino acid conjugates that are stable to purine nucleoside phosphorylase. *Org. Biomol. Chem.* **2020**, *18* (15), 2877−2885.

(32) da Silva, E. F. G.; Costa, B. P.; Nassr, M. T.; de Souza Basso, B.; Bastos, M. S.; Antunes, G. L.; Reghelin, C. K.; Garcia, M. C. R.; Schneider Levorse, V. G.; Carlessi, L. P.; et al. Therapeutic effect of uridine phosphorylase 1 (UPP1) inhibitor on liver fibrosis in vitro and in vivo. *Eur. J. Pharmacol.* **2021**, *890*, No. 173670.

(33) Yaku, K.; Okabe, K.; Gulshan, M.; Takatsu, K.; Okamoto, H.; Nakagawa, T. Metabolism and biochemical properties of nicotinamide adenine dinucleotide (NAD) analogs, nicotinamide guanine dinucleotide (NGD) and nicotinamide hypoxanthine dinucleotide (NHD). *Sci. Rep.* **2019**, *9* (1), No. 13102, DOI: 10.1038/s41598-019-49547-6.